SAND2011-6998C

IMPACT OF TIME-VARYING LOADS ON THE PROGRAMMABLE PULSED POWER DRIVER CALLED GENESIS *

S.F. Glover[1ξ], J.-P. Davis[1], L.X. Schneider[1], K.W. Reed[1], G.E. Pena[1], C.A. Hall[1], H.L. Hanshaw[1], R.J. Hickman[1], K.C. Hodge[2], R.W. Lemke[1], J.M. Lehr[1], D.J. Lucero[2], D.H. McDaniel[1], J. G. Puissant[2], J.M. Rudys[1], M.E. Sceiford[1], S.J. Tullar[2], D.M. Van De Valde[3], F.E. White[2], L. K. Warne[1], R. S. Coats[1], W. A. Johnson[1]

[1]*Sandia National Laboratories, Albuquerque, NM 87185 USA*
[2]*Raytheon Ktech Corporation, Albuquerque, NM. 87123 USA*
[3]*EG&G, Albuquerque, NM 87107 USA*

Abstract

The success of dynamic materials properties research at Sandia National Laboratories has led to research into ultra-low impedance, compact pulsed power systems capable of multi-MA shaped current pulses with rise times ranging from 220-500 ns. The Genesis design consists of two hundred and forty 200 kV, 80 kA modules connected in parallel to a solid dielectric disk transmission line and is capable of producing 280 kbar of magnetic pressure (>500 kbar pressure in high Z materials) in a 1.75 nH, 20 mm wide stripline load. Stripline loads operating under these conditions expand during the experiment resulting in a time-varying load that can impact the performance and lifetime of the system. This paper provides analysis of time-varying stripline loads and the impact of these loads on system performance. Further, an approach to reduce dielectric stress levels through active damping is presented as a means to increase system reliability and lifetime.

I. INTRODUCTION

The goal of Genesis R&D is to create a technology base that enables the design of highly compact multi-MA current platforms with precision pulse shaping capabilities. Genesis technology development is directed at applications where physical footprint constraints are present and/or a high degree of pulse shaping is required. Genesis capabilities are consistent with the operating envelope required for a magnetic compression driver for dynamic materials experiments located at a synchrotron light source to enable time-resolved x-ray diffraction and imaging measurements.

The Genesis project has explored modular system architectures operating at aggressively high electric fields. This enables ultra-low inductance topologies which greatly reduces the system's operating voltage requirements when driving low-impedance loads. The highly modular nature enables precision pulse shaping through the use of genetic optimization techniques to select trigger times for individual modules. Genetic optimization also enables the minimization of peak voltage variations throughout the system to reduce stress and extend the system lifetime.

Performance of a system like Genesis can be significantly impacted by the load characteristics due to the tight coupling between the pulsed forming components and the load. The tight coupling is a result of the extremely low inductance, solid dielectric feed structure. This paper explores the response of the Genesis architecture to a time-varying load and the means to control the performance of this system through optimized triggering of the high current modules.

II. GENESIS SYSTEM

The multi-module Genesis system and its disk transmission line structure are depicted in Figure 1 and Figure 2 [1]. Modules contain the initial energy store and switches that are used to switch module current into the disk shaped transmission line. The transmission line provides an ultra-low impedance path from the parallel modules to the load through the use of a solid dielectric insulation system. Precision pulse shapes are achieved through temporal triggering of two hundred and forty high current modules, in 60 groups of four, to create pressure waves for dynamic materials experiments. Genesis was designed to produce waveforms up to 5 MA peak current, which develops 280 kbar of peak magnetic pressure in a 20 mm wide stripline load. A custom load assembly was designed to interface to the solid dielectric insulated disk plate structure at the center of the driver. The load inductance was determined through static analysis [2]. Use of solid dielectric insulation begins in the base of the high voltage modules and continues through the disk transmission line to a solid dielectric insulated stripline load. High-inductance insulator stacks are not required in the Genesis design as there is no need to separate fluids from each other or from a vacuum region as is typically found in conventional pulsed forming technologies such as Linear Transformer Drivers (LTDs) or the Z machine.

* Sandia National Laboratories is a multi-program laboratory managed and operated by Sandia Corporation, a wholly owned subsidiary of Lockheed Martin Corporation, for the U.S. Department of Energy's National Nuclear Security Administration under contract DE-AC04-94AL85000.
ξ email: sfglove@sandia.gov

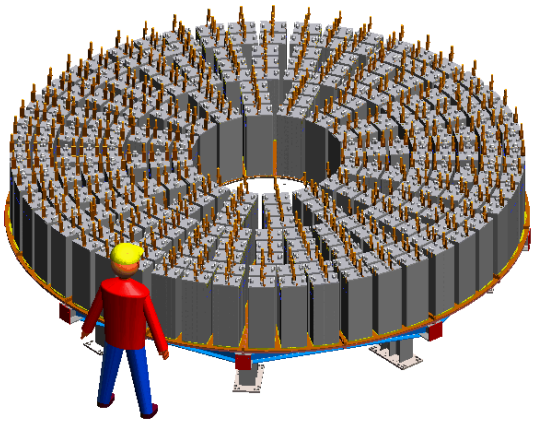

Figure 1. Programmable 5 MA Genesis system for dynamic materials experiments.

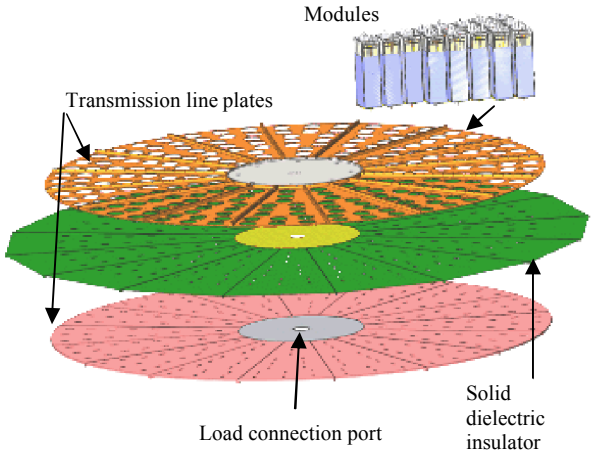

Figure 2. Genesis system components including high voltage modules and a solid dielectric insulated disk transmission line structure.

The transmission line consists of sixteen wedge shaped plates and a circular center section. Each wedge contains fifteen ports that allow for module connection and removal for maintenance. Fifteen of the modules are included in the figure above. The gap separating the disk transmission line plates was minimized to reduce circuit inductance, module charge voltage requirements, and system size. This is achieved through the use of a solid dielectric insulation system operating at a 564 kV/cm peak field. This number is calculated using the symmetry of the Genesis system, rotational averaging from shot to shot, and the waveforms from section IV. The stripline load, shown in Figure 3, is pre-mounted to interface hardware and installed in the center of the driver as indicated in Figure 2. The static inductance of this load out to a 5.2 cm radius is 1.75 nH [2].

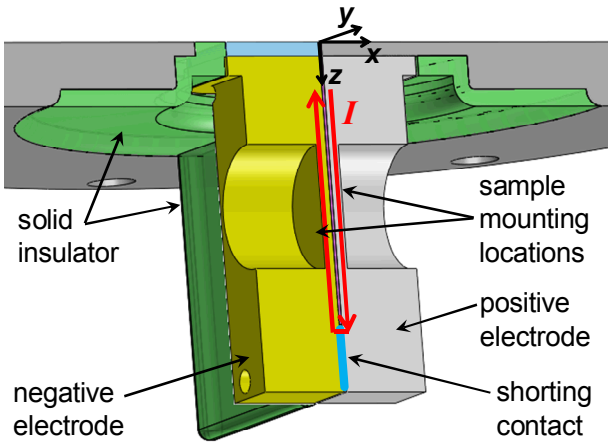

Figure 3. Isometric view from bottom of stripline load with counter-bores for mounting samples, indicating current path and coordinates referenced in Section III.

Figure 4 shows a cutaway view of the high current module which includes the outer housing, cabling, and gas lines. Each module contains two 80 nF capacitors, a High Current Electronics Institute (HCEI) switch [3] [4] [5], trigger resistor, and charge resistors. The capacitors and switch are arranged in the form of a two stage Marx Generator that can be charged to ±100 kV. One capacitor is connected electrically to the bottom of the module, the other to an electrode that protrudes out the bottom of the module. This electrode penetrates the solid insulator between the transmission line plates making electrical connection to the bottom transmission line plate.

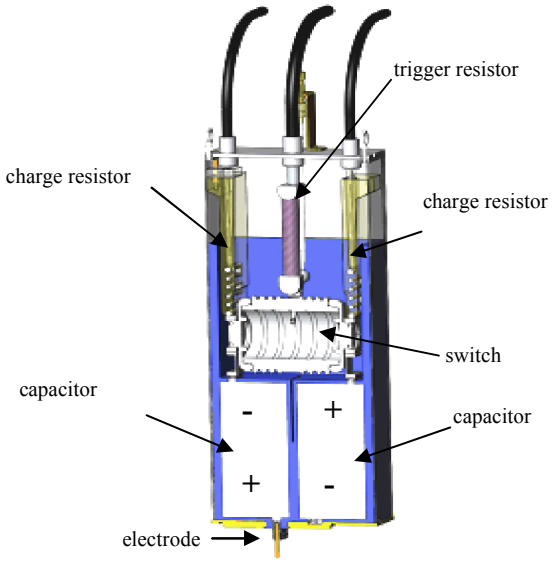

Figure 4. Module cutaway. The blue region is solid dielectric, allowing a more compact configuration.

A state equation based circuit model of the system shown in Figure 1 has been created in MATLAB [6] to model system performance during pulse shaping. One

sixteenth of the circuit diagram (one wedge of the transmission line plates) is depicted in Figure 5. The complete circuit diagram is circular in shape. In this model each module is represented as an RLC circuit with an ideal switch. Inclusion of transmission line elements accounts for the geometrical location of modules relative to each other and the load at the center of the system.

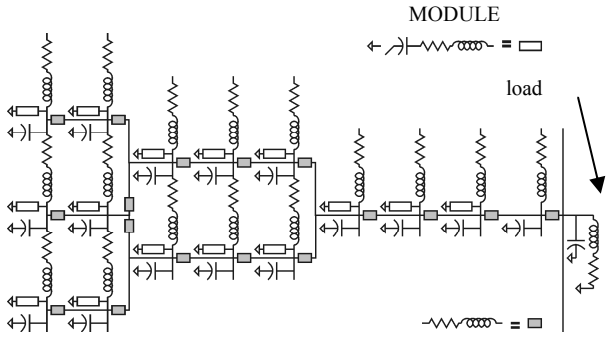

Figure 5. One sixteenth of the Genesis circuit diagram.

A genetic algorithm was used to determine optimum trigger times to produce precision pulse shapes for various dynamic materials experiments. This approach has been previously demonstrated [7] using the Genetic Optimization System Engineering Tool [8]. Current waveforms plotted in Figure 6 indicate both the range and flexibility of Genesis to produce shaped current pulses. Other pulse shapes are possible, including flat-top pulses and modified fall times.

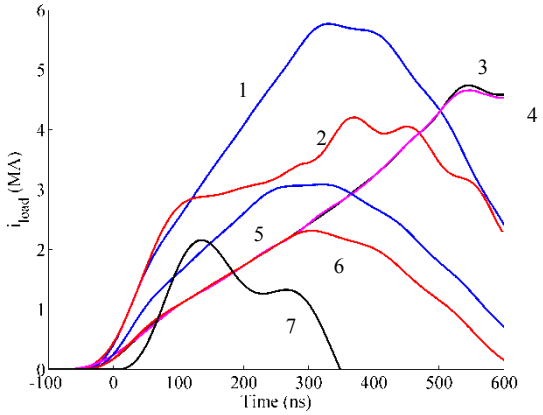

Figure 6. Example output pulse shapes for various materials: 1) Tungsten–5.7 MA 2) Iron–4 MA 3) Polypropylene–4.7 MA 4) Polypropylene–4.7 MA 5) Tungsten–3 MA 6) Tungsten–2 MA 7) 28 modules at t=0.

The simulations included in Figure 6 were generated from models using a static load inductance [9]. This earlier modeling did not account for movement of the stripline load during the primary pulse due to the high magnetic pressure generated at these current levels. It is this effect that allows energy from the current to be transmitted in the form of pressure to a material sample located on the outside surface of the stripline electrodes. Movement of the stripline results in a time-varying load impedance that can impact the performance of Genesis as discussed in the following sections.

III. DYNAMIC LOAD

The prototypical Genesis stripline load for dynamic materials studies consists of two parallel plate electrodes separated 432 μm by layers of Kapton® polyimide film and shorted at one end. The stripline configuration shown in Figure 3 is 20 mm wide, 50 mm long, and 12.5 mm thick, with a counter-bore machined in the back side down to 1-2 mm remaining thickness where material samples are mounted. The pulse of current flowing along the inner surfaces of the stripline (toward and away from the shorting contact) generates a time-varying magnetic field between the plates. As depicted in Figure 7, the resulting $\boldsymbol{J}\times\boldsymbol{B}$ Lorentz force manifests as a time-varying magnetic pressure on the material in the electrodes, resulting in a planar, time-ramped wave of mechanical stress propagating from the electrode into the sample material. The electrode material is Joule heated to gas and plasma states by the high current density, which lowers its conductivity by several orders of magnitude and greatly increases the rate at which magnetic field diffuses into the electrode. The mechanical stress wave propagates even faster than the magnetic diffusion front, allowing material dynamics experiments on ramp compression of the sample material that are decoupled from MHD effects such as Joule heating in the electrode.

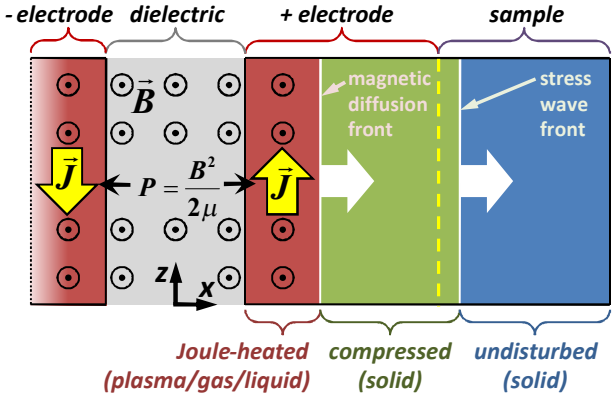

Figure 7. Schematic in *x*-*z* plane (*c.f.* Figure 3, flipped vertically so *z* axis points up) to illustrate generation of a mechanical stress wave and magnetic diffusion front in stripline electrodes. $\boldsymbol{J}$ is current density, $\boldsymbol{B}$ is magnetic field, P is magnetic pressure, and μ is permeability.

The electrical properties of the stripline load as seen by the rest of the machine vary in time as the magnetic field topology varies in time due to (1) acceleration of the electrodes away from each other by the magnetic pressure and (2) diffusion of the magnetic field into the electrodes. Computation of time-dependent magnetic-field topology requires magneto-hydrodynamic (MHD) simulations of the stripline during the current pulse. Though inherently a

3-D problem due to the stripline's finite length, stripline properties are reasonably well represented by a 2-D computational mesh lying in the *x*-*y* plane of Figure 3, positioned at the centerline of the counter-bores.

A 2-D simulation was performed using the finite-difference Alegra MHD code [10] with an experimental configuration relevant to a 5-MA peak current version of the tungsten waveform #1 in Figure 6. This consisted of 1.5-mm thick samples of tungsten mounted on aluminum electrodes in counter-bores of 1.0 mm remaining floor thickness. Though experiments typically use a different thickness sample or no sample on the opposite electrode, the present simulations used a symmetric stripline to simplify the problem. The simulation domain is semi-circular with the straight edge on the *x*-axis symmetry line, and includes both electrodes and surrounding vacuum region to ~7 cm radius. Figure 8 shows only that portion of the domain closest to the stripline at the time of peak applied current, $t = 250$ ns, (see Figure 10).

While the Genesis load has solid dielectric between the electrodes, the present calculations use a vacuum gap because wide-ranging equation-of-state (EOS) and conductivity models (encompassing states from solid through plasma and under compression) were not available for dielectric materials. The error due to this substitution is expected to be small and dominated by a hydrodynamic perturbation from thermal expansion of the dielectric material. The above 2-D MHD approach relies on wide-ranging aluminum EOS and conductivity models of high demonstrated accuracy [11], and has been successfully applied to vacuum-gap striplines at higher current densities [12].

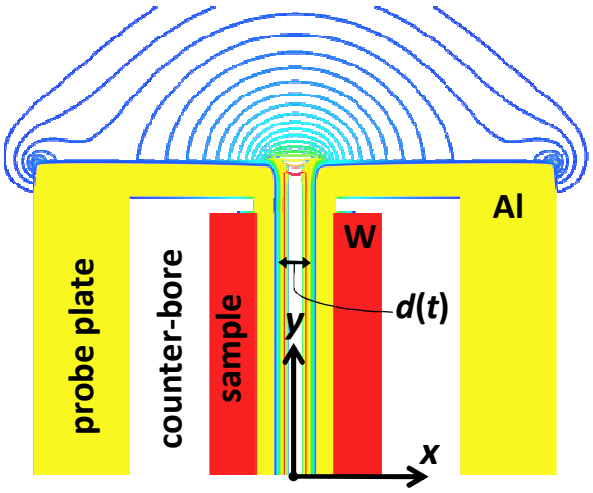

Figure 8. Close-up view of 2-D MHD result at $t = 250$ ns with line contours of B-field and filled contours of density (both on log scale) showing equivalent gap $d = 2x_{PEC}$

A 2-D MHD simulation driven by a prescribed load current $I(t)$ perpendicular to the plane of the mesh, as in Figure 8, can provide an accurate inductance history $L(t)$ by integrating the magnetic field energy in the mesh:

$$L(t) = \frac{h}{\mu\, I(t)^2} \int |\boldsymbol{B}(t)|^2\, dx\, dy \qquad (1)$$

where h is the height of the stripline up to the shorting contact, and the permeability $\mu \approx \mu_0$ for non-magnetic materials. The singularity as $I \rightarrow 0$ at current reversal (while finite magnetic field energy remains "frozen" into the electrode material) means this approach is not useful for determining load inductance during late-time ringing of Genesis. In fact, any method of obtaining inductance from electrical properties of the MHD mesh will fail for the same reason.

An alternative approach to compute $L(t)$ begins by extracting from the MHD solution at each time of interest the geometry of an equivalent perfect-electrical-conductor (PEC) stripline which has the same B-field at the gap centerline. Then a finite-difference, multi-block, alternating-direction implicit Poisson solver developed at Sandia [13] is used to compute a 2-D, normalized electrostatic solution of this PEC stripline with the electrodes at symmetric positive and negative electric potential. Finally, the traveling electro-magnetic (TEM) wave approximation (with duality between electrostatic and magnetostatic problems) is used to obtain inductance by integrating the electric field energy of the electrostatic solution:

$$L = \mu_0 h \left(\int |\boldsymbol{E}/V|^2\, dx\, dy \right)^{-1} \qquad (2)$$

where $\boldsymbol{E}/V$ is the normalized electric field

The only non-trivial part of the above procedure is determining the geometry of the equivalent PEC stripline. The problem is simplified considerably by use of a 1-D MHD simulation problem, represented in the 2-D Alegra MHD code by a mesh in the longitudinal plane (*x*-*z* plane in Figure 3; see also Figure 7) that is only one computational cell wide and defines a line through the thickness of one electrode and sample at the center of the counter-bore (the *x*-axis in Figure 8). The PEC geometry is then defined by the initial width (in *y*) and thickness (in *x*) of the electrodes, with a time-dependent equivalent gap $d(t)$ between the electrodes that accounts for material motion and B-field diffusion. This neglects the 2-D topology of motion and diffusion at the lateral edges of the stripline. The simplest method to determine the position x_{PEC} of the gap-facing boundary of an equivalent PEC electrode (for a symmetric stripline, $x_{PEC} = d/2$) is to integrate the B-field in the 1-D MHD solution:

$$x_{PEC} = x_0 + \frac{1}{B_y(x_0)} \int_{x_0}^{x_1} B_y(x)\, dx \qquad (3)$$

where x_0 is the gap-facing boundary and x_1 the outward-facing boundary of electrode material in the 1-D MHD problem, with the origin $x = 0$ at the gap centerline. This approach fails as $B_y(x_0) \rightarrow 0$ at current reversal, so a formulation was developed that tracks the position of the initial magnetic diffusion front while ensuring a

monotonic increase of separation between the equivalent PEC electrodes:

$$x_{\mathrm{PEC}} = x_{B\max} + \frac{1}{B_{\max}(x_{B\max})}\int_{x_{B\max}}^{x_1} B_y(x)\,dx \qquad (4)$$

where $x_{B\max}$ is the tracked position of the local maximum in B_y corresponding to the initial diffusion front. A typical PEC stripline with magnetostatic solution is shown in Figure 9, where initial positions of the electrodes are indicated by dashed lines.

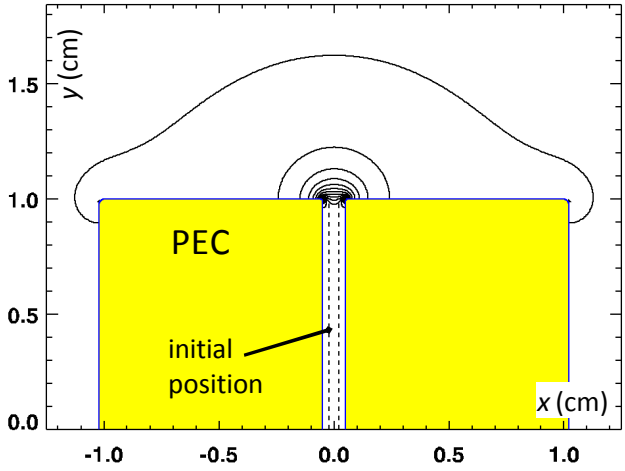

Figure 9. PEC stripline equivalent to MHD result in Figure 8, with d = 0.987 mm and linear-scale contours of B-field. Dashed lines indicate initial geometry.

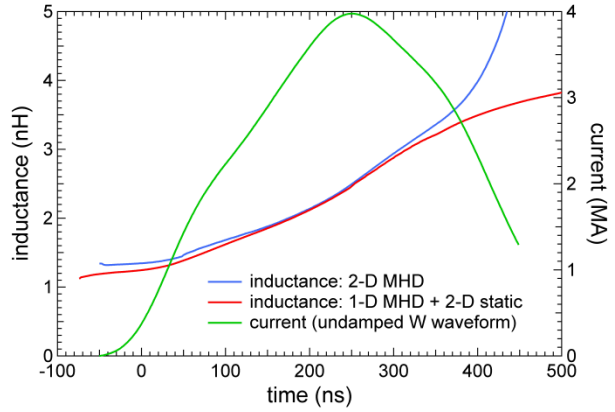

Figure 10 Comparison of $L(t)$ during initial pulse computed using the 2-D MHD and the approximate (1-D MHD + 2-D electrostatic) approaches.

The 1-D simulations are driven by an applied B-field, which is related to the stripline current I by a time dependent scale length $S(t)$:

$$I(t) = \frac{S(t)B_y(t)}{\mu_0} \qquad (5)$$

where S at each time is computed from the magnetostatic dual of the electrostatic solution. Thus iteration is required between the 1-D MHD and 2-D electrostatic calculations to arrive at a self-consistent result. The first iteration uses a constant S_0 given by the initial electrode geometry, while subsequent iterations use the last-computed $S(t)$. Convergence to 1% or better in $B_y(t)$ typically occurs between the third and fourth iterations. Figure 10 compares inductance computed using this approach [Eq. (4) and Eq. (5)] to the 2-D MHD result [Eq. (1)]; inductance of the latter begins to rise upon approaching the singularity near 500 ns, while the alternative approach, which matches the 2-D result well at earlier times, shows inductance flattening out as the diffusion front slows down.

The above calculation of inductance neglects coupling between the machine and the load; the inductance of the load seen by the machine affects the current delivered to the load by the machine. Since including the circuit model of Genesis in the Alegra simulation would be non-trivial, this coupling is addressed by iteration between the circuit model of Genesis and the inductance calculation.

IV. IMPACT OF TIME-VARYING LOAD

Implementing the time-varying load in the Genesis simulation was achieved by creating a lookup table of inductances versus time for a given load current. The challenge with this approach is that if the new load currents do not match the currents used to generate the time-varying inductance then the inductance calculations will be incorrect. The flexibility of Genesis pulse shaping helps eliminate this problem by changing trigger times to ensure that the new load current matches the current used to create the lookup table. With this in mind the steps to determine required switch trigger times with a time-varying load becomes:

- Create an ideal current pulse shape designed to produce shock-less loading of a material sample.
- Run an optimization on the Genesis circuit model with static load inductance, seeking an optimal match between the ideal pulse shape and the simulated pulse shape.
- Determine the dynamic load inductance using 1-D MHD with 2-D static analysis and the simulated current.
- Run the optimization again on the Genesis model, with a dynamic load inductance, fitting the pulse to the shape achieved in the second bullet above.

Ideal load current shapes for ramp compression can take a range of forms as indicated in Figure 6. In the examples that follow two extremes from that set were chosen for evaluation. One with a short rise time (Tungsten – W) and one with a long rise time (Polypropylene – PP). Figure 11 contains simulated waveforms for each material type utilizing a static load inductance. The ideal waveforms were created for these materials to maintain shock-less compression through a

particular sample thickness (1.5 mm for W, 1.0 mm for PP). They are ideal in the sense that, in the absence of MHD effects, and assuming perfect knowledge of the electrode and sample material response, the ramped stress wave would steepen into a shock wave at some distance greater than the sample thickness. In Figure 11, the ideal waveforms are plotted as red dashed curves that go from zero to peak current, blue traces are genetically optimized simulated results that seek a best fit to the ideal current while simultaneously seeking a solution that reduces late time reversal of voltage and current (active damping), and green traces are simulated waveforms that do not attempt to minimize reversal. In these simulations the active damping was much more effective with the Tungsten waveform where there were many more spare modules available at the end of the ideal waveform. Reducing the peak current of the polypropylene waveform would allow more modules to be available for active damping. Without a sufficient number of modules active damping is not possible as will be shown later in this paper. The fit to the ideal current is only lacking near $t = 0$ where dI/dt is limited by the impedances of the system. The number of modules used to achieve each waveform is different: undamped W–108, damped W–172, undamped PP–196, damped PP–208.

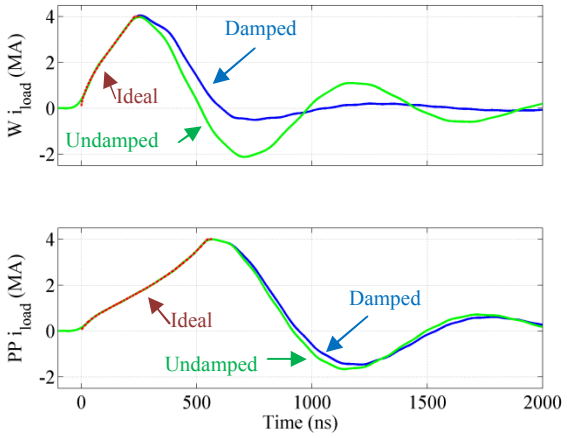

Figure 11. Load currents with static load inductance.

Active damping can be effective as indicated in Figure 11 and in Figure 12. Both current reversal and late time oscillations can be reduced allowing for a greater range of pressure-drive shapes for material science research. Furthermore, reduction of the electric fields between the transmission line plates, as seen in Figure 12, reduces dielectric stress, increasing reliability and lifetime.

When utilizing active damping, other components in the system, particularly the switches, capacitors, and module interfaces, may be stressed at higher levels. This is evident in Figure 13 where modules that are triggered late in time for active damping have larger peak currents because they are feeding the load as well as other modules that have reversed polarity.

Once the simulated load current shapes have been determined using a static load inductance, the methods in Section III are employed to estimate the time-varying load inductance specific to the given current shape. Figure 14 contains plots of the initial static inductance and the dynamic inductances estimated for the damped tungsten and polypropylene load current waveforms. From these estimates the inductance increases by over a factor of five at late times in the waveforms.

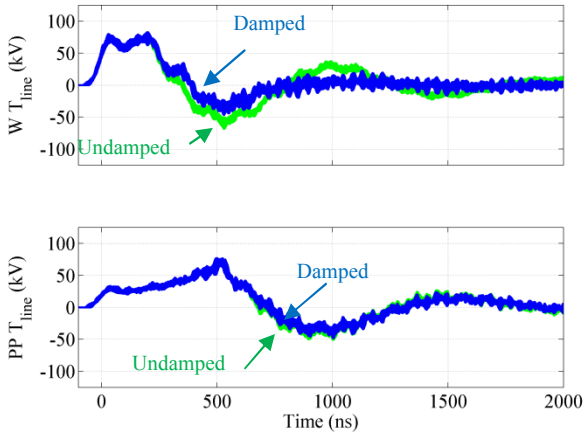

Figure 12. Transmission-line voltages with static load inductance.

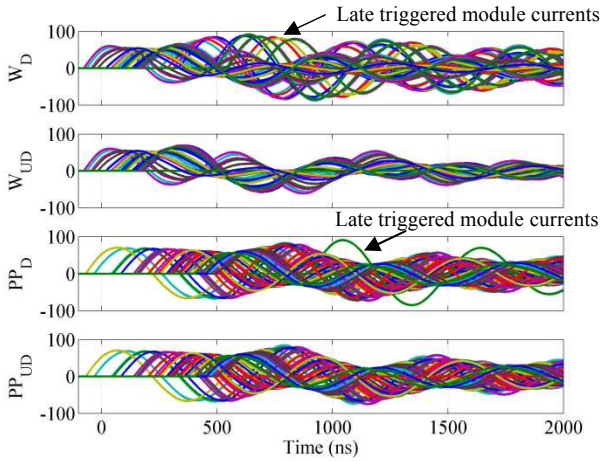

Figure 13. Module currents with static load inductance (D – damped, UD – undamped).

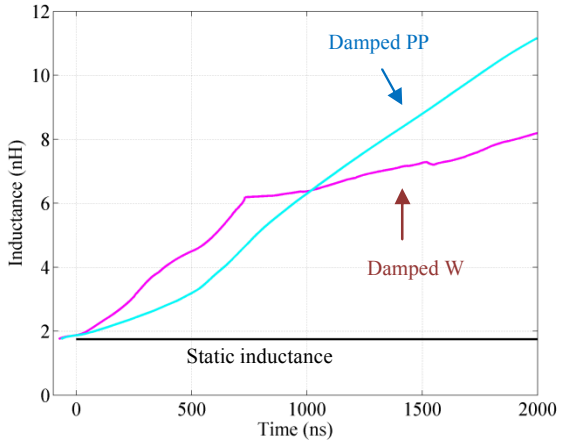

Figure 14. Static and dynamic load inductances for damped load current waveforms in Figure 11.

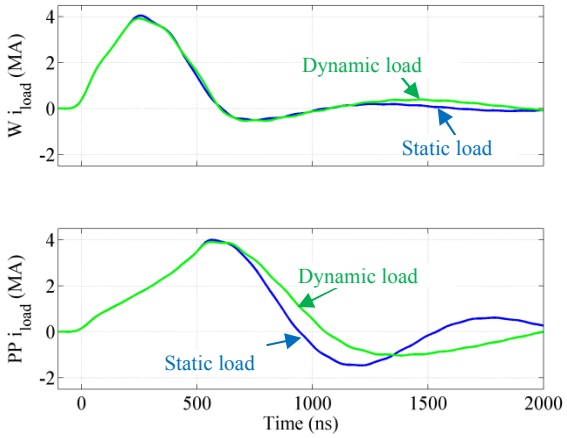

Figure 15. Damped load currents simulated with static and dynamic load inductance.

It must be kept in mind that the dynamic inductances in Figure 14 are only valid for specific load currents. Therefore to perform pulse shaping the simulations must be updated with the time-varying inductance and new trigger times must be identified that result in the original simulated currents. An alternative technique to genetic optimization for choosing the trigger times was utilized in this next step. This technique approach is iterative, utilizes a fixed order to the triggering of the modules, and therefore only determines the trigger times that provide pulse shaping. The downside of this technique is that the ability to minimize multiple constraints is lost. Future work will look at using genetic or other optimization approaches for this next step in an attempt to minimize stresses in the system. Plotted in Figure 15 are the load currents simulated using the original static load inductance and the new dynamic load inductance. Early in time over the range of the ideal waveform good agreement is achieved. The dynamic load had a larger impact later in time. This is partially caused by the pulse shape fitting method and the number of available modules. With the dynamic load the number of required modules necessary to achieve the desired current pulse shape increased. The tungsten waveform with dynamic load used 180 modules up to 849 ns the remaining modules were triggered at 1993 ns. The polypropylene waveform with dynamic load used 200 modules up to 489 ns, the remaining modules were triggered between 1000 ns and 1300 ns. Results in Figure 15 indicate that more modules would be necessary to improve the active damping with this polypropylene waveform. Two ways to achieve this are to design a larger system or reduce the amplitude of the ideal waveform.

Increasing load inductance does result in greater dielectric stresses in the transmission line as can be seen in Figure 16 where peak voltages that were significantly lower than 100 kV now reach and even exceed 100 kV. The effect is even greater when comparing the reversal voltages.

Some module currents also increase in this simulation as shown in Figure 17. This is primarily due to the choice of trigger times and the larger transmission-line plate voltage reversal that appears with the dynamic load. A multi-constraint optimization technique may help alleviate this, but connecting late-time modules across the transmission-line plate at a larger voltage reversal point impact the amplitude of module currents. Table 1 provides a list of the more significant stresses in the system allowing for the impact of a dynamic load to be better understood. The largest impact was on voltage reversal in the transmission line plates where increases over 100% were observed for the tungsten.

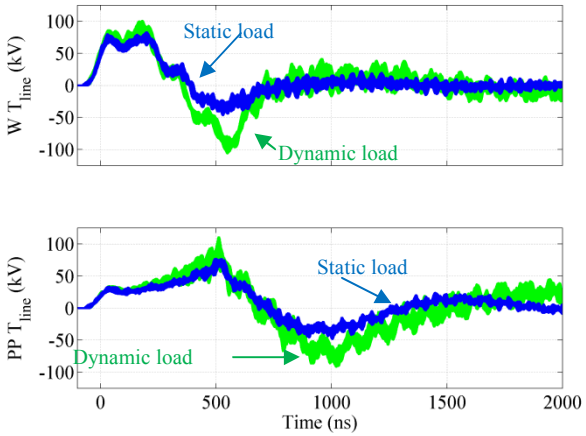

Figure 16. Damped transmission line voltages simulated with static and dynamic load inductance.

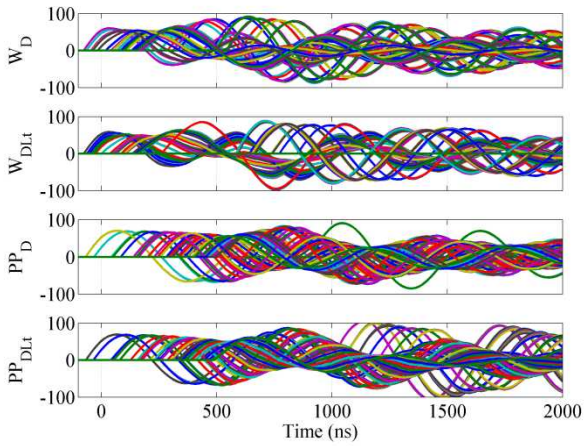

Figure 17. Module currents simulated with static and dynamic load inductance (Lt – time-varying inductance).

The analysis and simulation presented in this section demonstrate the flexibility and performance of the technologies being advanced for low impedance pulsed power current adders, such as Genesis. Furthermore the requirement for high fidelity models becomes immediately apparent. Research continues to address these needs relative to both the time-varying loads discussed in this paper and other critical system components, such as the switch, discussed in [15].

Table 1. System stress levels[1]

	Dielectric		Module[2]	Capacitor[2]	
	Peak Voltage (kV)	Peak Reversal (kV)	Peak Current (kA)	Peak Reversal	
W_D	82.7	46.7	92.2	109%	Max
	77.0	37.9	66.2	68.3%	Avg
	68.7	28.4	51.3	27.6%	Min
W_{DLt}	100.8	106.2	88.6	128.9%	Max
	90.2	94.8	49.8	75.7%	Avg
	79.0	84.9	63.3	35.7%	Min
PP_D	76.9	48.4	91.0	110.3	Max
	71.6	41.0	63.5	67.2	Avg
	65.6	31.7	53.0	36.1	Min
PP_{DLt}	110.9	91.7	105.1	137.2%	Max
	87.0	81.4	64.6	80.7%	Avg
	69.9	71.7	47.8	39.6%	Min

[1] Initial charge voltage was ±100 kV, and the spacing between transmission line plates was 1.27 mm.
[2] Some modules were not triggered, only triggered modules were used in these calculations.

V. CONCLUSION

The dynamic behavior of the stripline and material sample which form the load for Genesis impacts the performance of this system in a complex manner. A method has been presented which quantifies this dynamic interaction and provides a prediction of the time-varying load inductance using 1-D MHD with 2-D static analysis. Module triggering sequences, capable of producing precision pressure profiles, were determined for tungsten and polypropylene material samples. The flexibility and broad operating range of Genesis are demonstrated by the ability to account for the dynamically changing loads. Reduction in Genesis dielectric stress by multiobjective optimization achieved significant results by reducing voltage reversal in simulations with static load inductances. Further research is required to demonstrate electric field reductions when accounting for dynamic loads.

VI. ACKNOWLEDGEMENTS

The authors would like to thank: H.D. Anderson, H.L. Brown, M.L. Horry, M.D. Knudson, M.J. Madlener, G. Neau, K. Prestwich, V. Romero, S.D. Sudhoff, and R. White for their support, insight, and valuable discussions regarding this project. The authors also gratefully acknowledge valuable contributions from their colleagues at Sandia National Laboratories, Raytheon Ktech Corporation, EG&G, L-3 Communications, and Purdue University.

VII. REFERENCES

[1] SolidWorks 3D CAD Software, Dassault Systèmes SolidWorks Corp., 300 Baker Avenue, Concord, MA 01742, USA, www.solidworks.com
[2] L. K. Warne, R. S. Coats, R. E. Jorgenson, and W. A. Johnson, "Load Impedance and Current Distribution for Pulsed Power Device," Sandia National Laboratories Internal Report, December 19, 2007, LKWarne@sandia.gov.
[3] B.M. Kovalchuk, et al. "Multi gap switch for Marx generators," Pulsed Power Plasma Science Conference, pp. 1739-1742, June, 2001.
[4] M.G. Mazarakis, et al., "High current, 0.5 MA, fast, 100ns linear transformer driver experiments," Physical Review Special Topics – Accelerators and Beams, 12, 050401 2009.
[5] J. R. Woodworth, et al., "Low-inductance gas switches for linear transformer drivers," Physical Review Special Topics – Accelerators and Beams 12, 060401, 2009.
[6] MATLAB The Language of Technical Computing, The MathWorks, Inc., 3 Apple Hill Drive, Natick, MA 01760-2098 USA, info@mathworks.com.
[7] S.F. Glover, et al., "Genetic optimization for pulsed power system configuration," IEEE Transactions on Plasma Science, Vol. 37, No. 2, pp. 339-346, February 2009.
[8] S.D. Sudhoff and Y. Lee, "Energy Systems Analysis Consortium (ESAC) Genetic Optimization System Engineering Tool, v. 2.2 Manual," School of Electrical and Computer Engineering, Purdue Univ., West Lafayette, IN., 47907. sudhoff@ecn.purdue.edu.
[9] S.F. Glover, et al., "Genesis: A 5 MA programmable pulsed power driver for isentropic compression experiments," IEEE Transactions on Plasma Science, Vol. 38, No. 1, pp. 2620-2626, October, 2010.
[10] A. C. Robinson, et al., "ALEGRA: An Arbitrary Lagrangian-Eulerian Multimaterial, Multiphysics Code," AIAA 2008-1235, 46th AIAA Aerospace Sciences Meeting and Exhibit, 2008.
[11] R. W. Lemke, et al., "Characterization of magnetically accelerated flyer plates," *Physics of Plasmas*, Vol. 10, No. 4, pp. 1092-1099, April 2003.
[12] R. W. Lemke, M. D. Knudson, and J-P. Davis, "Magnetically driven hyper-velocity launch capability at the Sandia Z accelerator," *International Journal of Impact Engineering*, Vol. 38, pp. 480-485, 2011.
[13] D. B. Seidel, private communication (dbseide@sandia.gov).
[14] S.F. Glover, et al., "Impact of time varying loads on the programmable pulsed power driver called Genesis," 18th IEEE International Pulsed Power Conference, June 2011.
[15] S.F. Glover, et al., "Status of Genesis a 5 MA programmable pulsed power driver," 18th IEEE International Pulsed Power Conference, June 2011.